

# Aircraft turbulence measurements to estimate surface heat fluxes from the mixed layer variance methods over semi-arid grassland

KOTANI Ayumi<sup>1</sup> and SUGITA Michiaki<sup>1</sup>

<sup>1</sup> Graduate School of Life and Environmental Sciences, University of Tsukuba, Tsukuba, Japan

Key words: Mixed layer, Aircraft observation, Variance method

## I Introduction

The aircraft observation has an advantage in deriving area-averaged values and detecting the spatial variability, although it requires careful instrument settings and data processing especially in case of using wind data in eddy correlation method to evaluate fluxes (e.g., Lenschow, 1986). The variance methods to estimate surface fluxes from the associated variances measurements in the surface or mixed layer on the other hand are appealing in this context because it is possible to derive surface fluxes without observing wind velocity. The variance methods have been applied to surface layer and produced satisfied results (e.g., Wesely, 1988). On the contrary, convective boundary layer, where the flux-variance relationship is not fully understood and established yet. Until now, only a limited number of studies are available on this topic with examples of Asanuma (1996) from aircraft and Sugita and Kawakubo (2003) from tower observation of the lower half of the convective boundary layer.

In this study, investigation of the mixed layer variance methods by means of airborne data is presented.

## II Data

### 1. Aircraft observation

The temperature turbulence data were obtained by aircraft observation carried out from June to October of 2003 as a part of the field observation of RAISE (Rangelands Atmosphere-Hydrosphere-Biosphere Interaction Study Experiment in Northeastern Asia). The RAISE study area covers the Kherlen River basin, the arid to semi-arid region in northeastern Mongolia, with a boreal forest in northern and upper watershed and grassland (Steppe) area towards the southern and downstream part.

The instruments were installed to a wing of an aircraft, AN2 to measure scalar variables of the air temperature and humidity with a fine thermocouple (CC-type) and a Krypton hygrometer (KH20, Campbell Scientific Inc.). The data were sampled at 10 Hz. Also positioning information was obtained by a GPS receiver. The flight path covered the experimental area and several heights of 100, 200, 500 and 1,000 m were flown repeatedly above the ground observation site (see below). Although each path length is different depending on the weather condition, those with flight paths longer than 5 km, which is equivalent to 100 s of averaging time, and with the standard deviation of the flight level within 30 m have been selected for analysis. For each path, the data

have been processed to remove a trend by a linear regression method before the analysis.

### 2. Ground based observation

Within the grassland area, one flux station and four automatic weather stations (AWSs) were in operation during the flights. At the flux stations, the surface fluxes of sensible heat and water vapor were directly measured by the eddy correlation method every 30 minutes. Since the eddy correlation flux data showed the energy imbalance, the energy shortage has been distributed into the turbulence energy flux by keeping Bowen ratio (Twine *et al.*, 2000) for this analysis.

The surface fluxes of AWS sites were estimated by applying the bulk similarity method, with meteorological data such as air temperature, humidity, wind speed and radiation. The bulk transfer coefficients have been evaluated based on the data sets obtained through a flux measurement carried out for a few days at each of the AWS sites during the field campaign (Kojima, 2004).

## III Results

In the convective boundary layer (CBL), turbulence statistics were found to follow the convective (or mixed-layer) scaling. The aircraft observed temperature variance  $\sigma_\theta$  scaled with  $T^*$  ( $= [\overline{w'\theta_0}]^2 (gh)^{-1}$ )<sup>1/3</sup>,  $\theta$  is potential temperature and  $\overline{w'\theta_0}$  is surface temperature flux, and  $h_i$  is boundary layer height) plotted against  $\xi = zh_i^{-1}$ , where  $z$  is sensor height in Fig. 1 with some formulation proposed in previous studies. The boundary layer height  $h_i$  was estimated by the method proposed by Liu and Ohtaki (1997) with spectral data of horizontal velocity observed at the flux

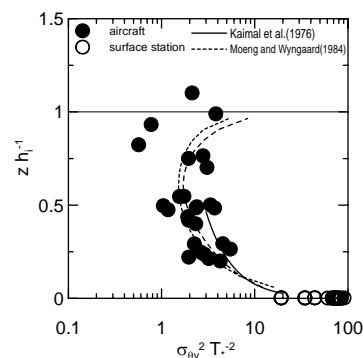


Fig. 1 Vertical profile of normalized variance of  $\theta$ .

stations. The height of CBL is around 700-1,200 m. The observed values follow the functional forms in general except for the upper part of CBL, where the scatter is relatively larger probably because of the entrainment flux dominating near the inversion layer. The effect of entrainment flux might appear on the vertical profile of temperature skewness and correlation between temperature and humidity (not shown). Thus, those data were not used for variance methods.

Kaimal *et al.* (1976) obtained with observation data for  $0.1 \leq zh_i^{-1} \leq 0.5$ ,

$$\sigma_\theta^2 T_*^{-2} \approx 1.8\xi^{-2/3} \quad (1)$$

Others have included the whole boundary layer diffusion process with the top-down and bottom-up (TDBU) model (Moeng and Wyngaard, 1984), which separates the source of the boundary layer diffusion process into the surface and the inversion origins, and can be written in general form by Asanuma (1996),

$$\sigma_\theta^2 = \left(\frac{w'\theta'_h}{v_h}\right)^2 f_t(\xi) + 2\left(\frac{w'\theta'_h}{v_h} \frac{w'\theta'_0}{v_0}\right) f_{tb}(\xi) + \left(\frac{w'\theta'_0}{v_0}\right)^2 f_b(\xi) \quad (2)$$

where  $v_h$  and  $v_0$  are the velocity scale at the inversion base and at the surface, respectively. These scales should include the effect of surface shear and the convective (buoyant) forcing. Therefore available selection can be the friction velocity  $u_*$ , convective velocity  $w_*$  and their combination such as  $v_* = (w_*^3 + 8u_*^3)^{1/3}$  (Driedonks, 1982), for example. Since velocity was not observed in the present study,  $u_*$  was estimated with the Rossby-number similarity which gives relation between the surface stress and the geostrophic wind. The geostrophic wind speed can be evaluated with the gradient of geopotential height of the six hourly NCEP/NCAR reanalysis data (Kalney *et al.*, 1996). The universal function  $f_t, f_{tb}$  and  $f_b$  are written as follows,

$$f_t = a_1(1-\xi)^{a_2}, \quad f_{tb} = a_3(1-\xi)^{a_4} \xi^{a_5}, \quad f_b = a_6 \xi^{a_7} \quad (3)$$

where  $a_1$  to  $a_7$  are the constants to be determined experimentally.

By changing the combination of the velocity scale and the entrainment model, several selections of the test under various conditions are possible. Here, two combinations shown in Table 1 have been tested. Eqs. (1) and (2) were rewritten to obtain surface flux  $w'\theta'_0$  by following Sugita and Kawakubo (2003). As mentioned, the constants in eq. (3) are still not well established and need further studies. As such in the present analysis, first those constants previously proposed were applied and then they were calibrated with the current data sets.

The calibration was performed in the same manner as Sugita and Kawakubo (2003), where powers  $a_2, a_4, a_5$

and  $a_7$  in eq. (3) are retained and the other coefficients were changed at a small step until the root mean square (rms) difference between the estimated flux and reference flux became the smallest.

The result before and after the local calibration is shown in Fig. 2 and Table 1. As shown, the rms difference of the sensible heat flux was improved to about  $35 \text{ Wm}^{-2}$  with the calibration. In the case of the convective scaling for lower half of ABL (Fig. 2, left), the original constants (Kaimal *et al.*, 1976) produced the same level of difference with the calibrated constant, which might reveal that the convective scaling of the lower boundary layer is rigid for various surface types. For the TDBU-based formulation, those combinations of velocity scale gave little difference in the results, which agreed with previous studies (Asanuma, 1996). These results with the calibration are comparable to those obtained by the tower-based data of Sugita and Kawakubo (2003).

**Table 1 Result of variance method.**

Equation number	rms difference ( $\text{Wm}^{-2}$ )*1	
Combination of $v_0, v_h$	Aircraft	Tower**2
(1)	40.5 → 37.2	41.0
(2a) $v_0 = v_h = w_*$	82.0 → 34.1	60.9 → 40.3
(2b) $v_0 = v_*, v_h = w_*$	106.3 → 34.4	136.0 → 44.1

\*1 original constant      calibrated constant  
\*2 Sugita and Kawakubo (2003)

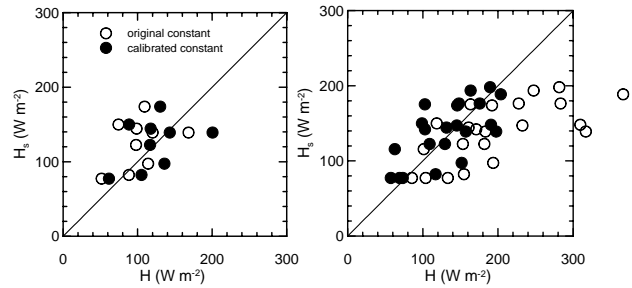


**Fig. 2 Comparison of H by variance method and  $H_s$  by eddy correlation method at flux site. (left: eq. (1), right: eq. (2a) of Table 1)**

The variance equations with these calibrated coefficients were applied to the AWS site, where fluxes have been derived by the bulk similarity method with the meteorological data. The sensible heat flux by variance method and the bulk method at three AWS sites is compared in Fig. 3. The rms difference between these fluxes is  $68 \text{ Wm}^{-2}$ , which is rather large since it might contain the error of referenced surface fluxes and thus require further studies.

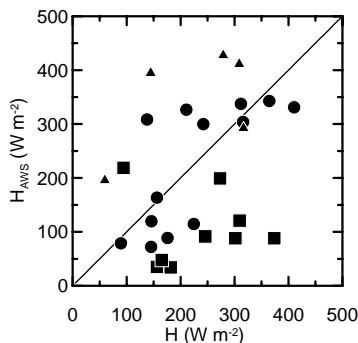


**Fig. 3 Comparison of H by variance method and H<sub>AWS</sub> by bulk similarity method at AWS site. (eq. (2a) of Table 1)**

#### IV Conclusions

Turbulence data obtained by aircraft observations in CBL were analyzed to estimate the surface fluxes by means of variance methods. Observed temperature variances followed in general the CBL scaling and produced the surface heat fluxes with about 80 Wm<sup>-2</sup> of rms difference against ground based eddy correlation fluxes. The calibration of the experimentally determined coefficients within the equations reduced the difference to 40 Wm<sup>-2</sup>. This rather large error relative to reference value is partly due to uncertainty of other parameters such as CBL height or regional friction velocity. This degree of error, however, is comparable to tower based measurement.

Finally, these equations with the locally calibrated coefficients were applied to the data over the other areas with the AWSs, where surface fluxes have been obtained by the bulk similarity method. Although the difference increased, it was probably because of the larger uncertainty of the ground based fluxes derived indirectly.

#### References

- Asanuma, J. (1996): Turbulence Variance Characteristics in the Unstable Atmospheric Boundary Layer above Flat Pine Forest. *Ph. D. Thesis, Cornell University*, 118 p.
- Driedonks, A. G. M. (1982): Models and Observation of the Growth of the Atmospheric Boundary Layer. *Boundary-Layer Meteorol.*, **85**, 497-504.
- Kaimal, J. C., Wyngaard, J. C., Haugan, D. A., Cote, O. R. and Izumi, Y. (1976): Turbulence Structure in the Convective Boundary Layer. *J. Atmos. Sci.*, **33**, 637-662.
- Kalney, E. and coauthors (1996): The NCEP/NCAR 40-year reanalysis project, *Bull. Amer. Meteor. Soc.*, **74**, 789-799.
- Kojima, T. (2004): The investigation of the factors which govern evapotranspiration of Kherlen River basin in Mongolia. *MSc Thesis, University of Tsukuba*, 85p.
- Lenschow, D. H. (1986): Aircraft Measurements in the Planetary Boundary Layer. In *Probing the Atmospheric Boundary Layer*, Am. Meteorol. Soc., Boston, 5-18.
- Liu, X. and Ohtaki, E. (1997): An Independent Method to Determine the Height of the Mixed Layer. *Boundary-Layer Meteorol.*, **85**, 497-504.
- Moeng, C-H. and Wyngaard, J. C. (1984): A Comparison of Shear- and Buoyancy-Driven Planetary Boundary Layer Flow. *J. Atmos. Sci.*, **41**, 3161-3169.
- Sugita, M. and Kawakubo, N. (2003): Surface and Mixed-layer Variance Methods to Estimate Regional Sensible Heat Flux at the Surface. *Boundary-Layer Meteorol.*, **106**, 117-145.
- Twine, T. E., Kustas, W. P., Norman, J. M., Cook, D. R., Houser, P. R., Meyers, T. P., Prueger, J. H., Starks, P. J. and Wesely, M. L. (2000): Correcting eddy-covariance flux underestimates over a grassland. *Agric. For. Meteorol.*, **103**, 279-300.
- Wesely, M. (1988): Use of Variance Techniques to Measure Dry Air-surface Exchange Rates. *J. Atmos. Sci.*, **44**, 13-31.